X-ray-absorption spectroscopy of ZnTe, CdTe, and HgTe: Experimental and theoretical study of near-edge structures

A. Kisiel,* G. Dalba, and P. Fornasini
Dipartimento di Fisica, Università degli Studi di Trento, I-38050 Povo (Trento), Italy

M. Podgórny and J. Oleszkiewicz
Instytut Fizyki, Uniwersytet Jagielloński, Reymonta 4, PL-30-059 Kraków, Poland

F. Rocca
Centro di Fisica degli Stati Aggregati ed Impianto Ionico, Consiglio Nazionale delle Ricerche, I-38050 Povo (Trento), Italy

E. Burattini
Laboratori Nazionali di Frascati, Istituto Nazionale di Fisica Nucleare, via Enrico Fermi, Cassella Postale 13, I-00044 Frascati (Roma), Italy

(Received 3 May 1988)

X-ray near-edge absorption structure for ZnTe, CdTe, and HgTe has been studied with the use of synchrotron radiation. The L_1, L_2, and L_3 edges have been analyzed for Cd and Te in CdTe, as well as the L_1 and L_3 edges for Te in ZnTe and HgTe and the K edge of Zn in ZnTe. The experimental results are compared with absorption spectra which have been calculated on the basis of conduction-band state densities obtained from self-consistent linear muffin-tin-orbital calculations. A comparison of the experimental and theoretical results yields in most cases a good quantitative agreement, in particular for all L_1 and K edges analyzed. Due to deficiencies of the theoretical model, not quite so satisfactory results have been obtained for Cd L_2 and L_3 edges. In general, the results substantiate the opinion that the near-edge x-ray absorption for semiconductors can be satisfactorily described within the one-electron approximation, although for L_2 and L_3 edges the pre-edge region seems to be influenced by excitonic many-body effects, and that the combination of x-ray-absorption spectroscopy (XAS) and band-structure calculations constitutes a powerful tool for investigations of the empty states of these materials.

I. INTRODUCTION

Many efforts have been made in the 1970s to develop the photoelectron spectroscopy for studying occupied electronic states in condensed matter. Recently, a similar development is observed in the studies of unoccupied electronic states. The importance of such studies for our understanding of the nature of excited states in solids need not be stressed. Techniques such as optical and core-level reflection spectroscopy,[1] bremsstrahlung isochromat spectroscopy[2–11] (BIS), or rather old techniques of x-ray emission[12,13] and absorption[14–24] spectroscopy (XAS) are being focused on the analysis of the empty-band density of states (DOS). All the above-mentioned methods supply valuable, complementary results that should describe, in a direct or indirect way, the conduction-band (CB) DOS. The low-energy optical reflection spectrum has a resolving power much higher than other adequate methods (better than 0.1 eV),[1] however it delivers rather limited information on the CB DOS because the absorption mechanism for this technique is governed by van Hove singularities[1,25] that depend on the shape of the joint density of states of valence and conduction bands rather than on the CB DOS itself. BIS is a relatively new, outstanding method used recently to study empty electronic states in solid state; it reflects directly the total CB DOS with an acceptable resolution of $\sim$0.7 eV (Ref. 5) and can be also used to trace the band dispersions in ordered crystals. However, the price paid for this advantage is a long acquisition time. Besides, BIS results contain no information on the origin and nature of the observed DOS. XAS does not provide any information on band dispersions and is characterized by a resolving power which is usually lower than that of BIS and decreases with increasing transition energy and atomic number of the absorbing element; it can nevertheless be applied with success to the analysis of the CB DOS due to the several favorable features of XAS spectrometers installed on synchrotron radiation facilities. These features include very high accuracy of measurements, high sensitivity, very short acquisition time, and lack of limitations on the studied energy range.[26,27] Moreover, the technique by itself is selective with respect to atomic species and to the component of the DOS. In this paper we will make substantial use of these features, comparing the experimental spectra with calculated l– and atom-type–decomposed densities of states.

Solid-state XAS is commonly studied in two overlap-

ping energy ranges that correspond respectively to a dominant influence of electronic band structure [x-ray-absorption near-edge structure (XANES)] and of scattering of almost-free electrons on the neighboring atoms [extended x-ray-absorption fine structure (EXAFS)]. The applicability of the one-electron and/or many-body approximations in the analysis and interpretation of XANES has been a subject of lively debate recently. Gupta and Freeman[17] have shown that general properties of the L_2,L_3 edges of Mg can be satisfactorily described by the CB DOS calculated within a one-electron approximation up to 2–3 eV above the Fermi level. They have ascertained that in that case the contribution of many-body effects[18] does not play any significant role. A good qualitative agreement with experiment has also been reported by McCaffrey and Papanconstantopoulos[28] for the Ca K edge up to 17 eV above the Fermi level and for both Ti and Fe K edges in Ti-Fe alloy.[29] The recent theoretical works of Müller *et al.*[20,21] for palladium, in which the muffin-tin (MT) approximation for the potential and a linear version of the augmented-plane-wave (APW) method specifically designed to cover a large energy range have been applied, confirm the prevailing contribution of the band-structure effects to the structures observed on K, L, and M edges of Pd even up to 200 eV above the Fermi level. According to Müller *et al.*,[21] a small deviation of the experimental results for Pd from the accurate single-particle calculations may originate from many-body effects. One such effect involves the filling of the core hole and the decay of the electron excited in the absorption process. This effect has been phenomenologically incorporated into calculations in Ref. 20 by convoluting the one-electron DOS with a Lorentzian broadening function, whose width has been taken equal to the sum of the inverse lifetimes of the core hole and excited electron.[20,21]

In the case of semiconductors and insulators one is faced anew with the question of what is mainly responsible for XANES: the conduction-band DOS structure calculated in a one-electron approximation or electron-hole excitations described at best in terms of many-body theory. Poumellec *et al.*[24] have suggested that in XANES of titanium and vanadium oxides the multielectron effects are predominant and thus the one-electron transition model is no longer satisfactory. On the other hand, the XAS measurements of Sagiura and Muramatsu[30] for FeS_2 and the results of one-electron calculations for this material included in the paper by Folkers *et al.*[6] compare quite well. It seems that the usefulness of one-electron concepts for interpretation of the XAS spectra of semiconductors has not yet been convincingly proved. It is the aim of this paper to demonstrate that, leaving for future discussion the question of the validity of a one-electron approximation for description of XAS of transition-metal compounds, the XANES spectra of typical zinc-blende II-VI compound semiconductors can be satisfactorily described in the frame of this theory. To accomplish this, we calculated the CB DOS in the energy range of $\sim$1.3 Ry above the bottom of the CB and we measured and analyzed the fine structure in the XANES energy range for the three most common II-VI compound semiconductors, ZnTe, CdTe, and HgTe, which are characterized, respectively, by a wide, medium, and narrow forbidden energy gap (2.27, 1.53, and -0.31 eV, respectively, at the room temperature).

The layout of the paper is as follows: Sec. II describes experimental details and the data-reduction method; in Sec. III an outline of theoretical calculations is presented, Sec. IV contains the discussion and Sec. V the conclusions.

II. EXPERIMENT AND RESULTS

A. XAS measurements

X-ray-absorption measurements have been carried out with the use of synchrotron radiation at ADONE Wiggler Facility in Frascati[31] utilizing the Si(111) channel-cut crystal monochromator. The original samples were high-purity monocrystalline ZnTe, CdTe, and HgTe ingots grown in the Institute of Physics of the Polish Academy of Sciences in Warsaw. To obtain thin specimens of a controlled thickness and homogeneity as required by the x-ray-absorption technique, the samples were finely powdered and deposited on polyacetate films.

XAS measurements have been carried out on the Te L_1 and L_3 edges for HgTe and ZnTe, the Zn K edge for ZnTe, and the Te and Cd L_1, L_2, and L_3 edges for CdTe. The energy resolution of an experimental setup of the type used by us is limited by a finite vertical divergence of the photon beam and a finite width of the rocking curve of the monochromating crystal. The resulting instrumental Gaussian broadening of the natural width of all measured edges has been estimated as $\sim$0.7 eV for Te and Cd L edges and as $\sim$1.7 eV for the Zn K edge.

The contribution of each edge to the absorption coefficient has been isolated by extrapolating the pre-edge region to higher energies by a Victoreen-like fit and by subtracting the fitted curve from the remaining experimental spectrum.[32] Figure 1 presents the results of measurements (after subtraction of the pre-edge contribution) and their first derivatives for the Te L_1 and L_3 edges in ZnTe, CdTe, and HgTe. Figures 2–4 show the spectra and their derivatives for the Te L_2 and the Cd L_1, L_2, and L_3 edges in CdTe and for the Zn K edge in ZnTe.

B. Experimental data reduction

As was mentioned above, XANES for metals is described satisfactorily by the one-electron approximation; however, the discrepancies between theory and experiment for higher energies above the Fermi level open the question of the quality of the theoretical approaches in this energy range. According to the Bloch theorem, for an ideal infinite crystal lattice the electronic band structure extends to infinity. In practical approaches to the band-structure calculations the number of bands calculated above the Fermi energy is limited by one reason or another, the size of the basis set being the ultimate technical limit. In general, for the reasons discussed in Sec. III A one is rather reluctant in attaching any direct physical meaning to the high-lying bands. Müller *et al.*[20,21]

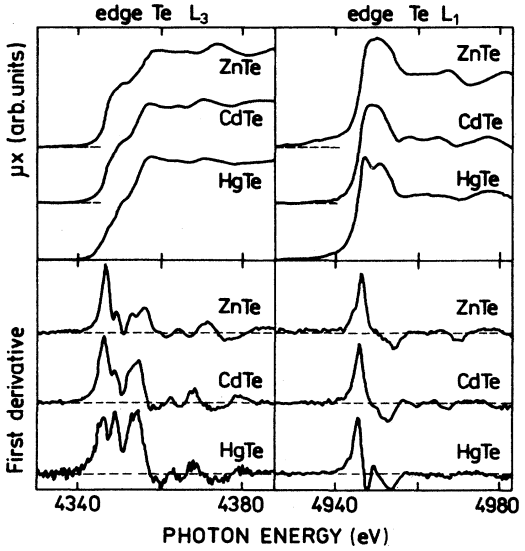

FIG. 1. Te L_3 and L_1 x-ray-absorption edges and their first derivatives for ZnTe, CdTe, and HgTe.

carried out their calculations for Pd up to approximately 200 eV but in most other available calculations the upper limit lies between 5 and 30 eV.[16,17,19,23,24] Hence, because of the limited applicability of the one-electron approximation mentioned above, and also because of the lack of a well-verified many-body theory, the explicit comparison of the theory with experiment in a whole XANES energy range is possible now only in very few cases [for instance, for Pd (Refs. 20 and 21)].

Considering the above difficulties we suggest a comparison of the experiment with accessible theoretical data using the procedure of experimental data reduction proposed at first by Parratt[33] for gaseous argon. Parratt suggested cutting off an upper part of the experimental spectrum and replacing it by an arctangent curve that according to Richtmyer *et al.*[34] corresponds to the shape of the x-ray-absorption edge of the free electrons. It has been shown in the Ref. 34 that this arctangent dependence describes very well the shape of the experimental absorption L edges of Au. Thereafter we express the total absorption coefficient μ_{tot} as

$$\mu_{\text{tot}}(E;\varepsilon)=\mu_{\text{BS}}(E;\varepsilon)+\mu_{\text{FE}}(E;\varepsilon)+\mu_{\text{os}} , \quad (1)$$

where μ_{BS} expresses a contribution to the total absorption from all transitions from the initial core state (assumed hereafter to possess a Lorentzian shape) to the empty CB DOS up to the energy limit ε that is arbitrarily defined by the extent of the theoretically calculated DOS; μ_{FE} expresses the contribution of the transitions from the same core state to the hypothetical continuum of the unoccupied free-electron-like states that extend above the energy limit ε; and μ_{OS} is due to transitions from other core states. The last contribution may be neglected if

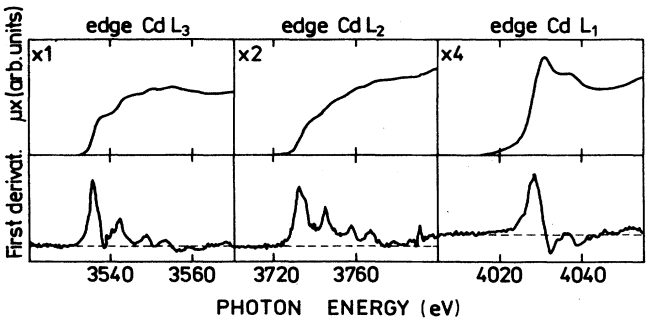

FIG. 3. Cd L_1, L_2, and L_3 edges and their first derivatives.

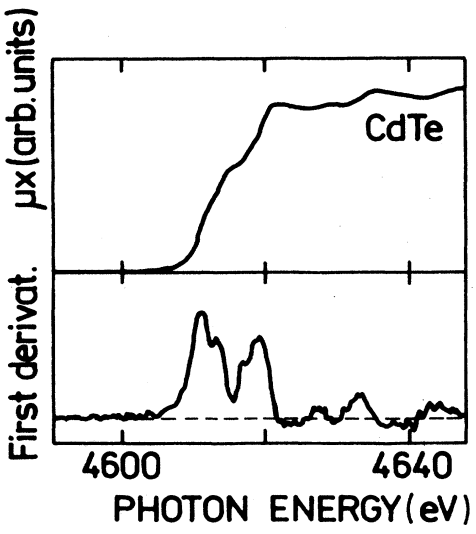

FIG. 2. Te L_2 edge for CdTe and its first derivative.

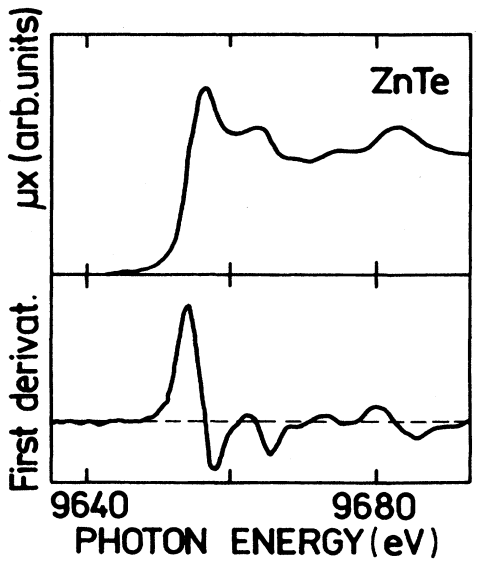

FIG. 4. Zn K edge and its first derivative.

every edge is analyzed independently, eliminating contributions from other edges by the Victoreen procedure.[32] The choice of the energy ε will be discussed later. Formula (1) means that the absorption coefficient μ_{BS}, related to the CB DOS calculated up to the energy limit ε, is augmented by the absorption coefficient correlated with the free-electron DOS above this limit. The term μ_{FE} in (1) is described by the integral[34,35]

$$\mu_{FE}(E;\varepsilon)=\int_{\varepsilon_\infty}\frac{B(E')}{1-4[(E-E')/\Gamma]^2}dE' , \tag{2}$$

where Γ is a natural Lorentzian half-width of the core state. Watanabe[36] has shown that $B(E)$ is a slowly decreasing monotonic function of energy. Hence, if we, after Richtmyer *et al.*,[34] (set $B(E)$=const, the integral (2) assumes a simple arctangent form

$$\mu_{FE}=\tfrac{1}{2}+\frac{1}{\pi}\tan^{-1}\left[\frac{2(E-\varepsilon)}{\Gamma}\right] . \tag{3}$$

Therefore, the band-structure contribution to the absorption coefficient can be written as

$$\mu_{BS}(E;\varepsilon)=\mu_{tot}(E)-\left[\frac{1}{2}+\frac{1}{\pi}\tan^{-1}\left[\frac{2(E-\varepsilon)}{\Gamma}\right]\right] . \tag{4}$$

This expression allows for a direct comparison of the reduced experimental data with a theoretical CB DOS convoluted with the Lorentz function describing the initial state and the Gaussian resulting from the experimental broadening. Figure 5 illustrates the experimental data-reduction procedure for two diverse types of x-ray edges. In formula (4) two parameters are necessary: the energy cutoff ε defined earlier and the Γ parameter which is a sum of the half-width of the Lorentzian initial state Γ_0, the experimental broadening Γ_G, and the broadening $\Delta\Gamma_x$ caused by the decrease of the lifetime of the excited states in the conductivity band with increasing electron energy. The last broadening estimated by Müller *et al.*[20,21] can be used to evaluate the total half-width at the cutoff energy ε. The correction estimated by Müller *et al.*[20] for low energies is not very large and might be neglected. We have used it, however, in all theoretical convolution calculations; consistently, it is included in our experimental data-reduction procedue. Figure 6

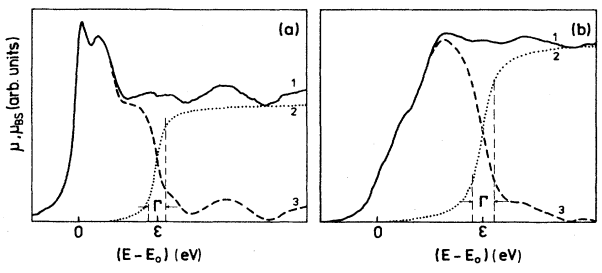

FIG. 5. The procedure of the experimental data reduction for two types of absorption edge. 1, experimental spectrum; 2, free-electron contribution at the energy cutoff.

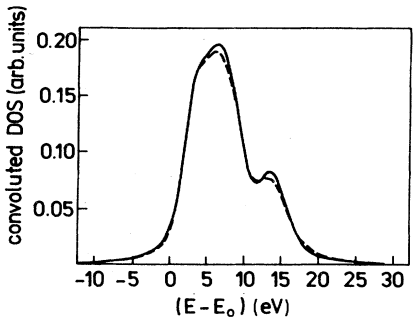

FIG. 6. Convoluted theoretical spectrum of the Te L_1 edge for CdTe with (solid line) and without (dashed line) the correction expressed by the Eq. (7).

shows the influence of this correction on the convoluted projected *p*-like CB DOS for the CdTe Te L_1 edge with realistic parameters Γ_0=2 eV and Γ_G=0.7 eV.

In the procedure of the experimental data-reduction we have used for HgTe ε=17 eV and for CdTe and ZnTe ε=15 eV [i.e., ~17 eV above the valence-band maximum (VBM)]. This choice of the cutoff energy was motivated by a decreasing accuracy of the band-structure calculations for higher conduction bands, as discussed in Sec. III A. The value of Γ_ε has been estimated using the approximate formula

$$\Gamma_\varepsilon\cong\Gamma_0+\tfrac{1}{2}\Gamma_G+\Delta\Gamma_\varepsilon \tag{5}$$

in which $\Gamma_0+\frac{1}{2}\Gamma_G$ is a compromise between the two components contributing to the line shape: the Lorentzian (natural width) and the Gaussian (instrumental width) ones.[35] The values of Γ_0 used in the data-reduction procedure are collected in Table I. They were taken after Savier monography (Ref. 35) and from Refs. 15 and 37. These values are significantly lower than those reported by Krause and Olivier.[38] They agree, however, much better with the values of Γ_0 that one obtains fitting our experimental results with formula (3) for ε=0.

The procedue of the experimental data reduction present above has two important practical features: it provides a direct comparison of the experimental data with available theoretical results whatever their energetical extent might be, and allows for a better identification

TABLE I. Parameters used in the procedure of experimental data reduction.

	Zn	Cd			Te		
	K	L_1	L_2	L_3	L_1	L_2	L_3
Γ_0 (eV)	1.40[a]	3.4[b]	2.15[c]	2.1[d]	2.5[e]	2.3[3]	2.3[e]

[a]Reference 37.
[b]Our estimate based on the approach used in Ref. 34.
[c]Reference 46.
[d]Reference 47.
[e]Reference 15.

of near-absorption-edge fine structures by scanning the experimental curve with different values of the parameter ε. It was, however, not necessary to use this virtue in the present paper due to the overall good agreement of the experimental and theoretical results.

III. THEORETICAL CALCULATIONS

A. Electronic structure

The electronic structures of CdTe, HgTe, and ZnTe were calculated using the self-consistent linear muffin-tin-orbital (LMTO) method.[39] The openness of the zinc-blende structure was dealt with in a customary way,[40] i.e., two "empty spheres" were placed at the positions $(\frac{1}{2},\frac{1}{2},\frac{1}{2})$ and $(\frac{3}{4},\frac{3}{4},\frac{3}{4})$ of the unit cell. Scalar relativistic corrections, very important in the case of HgTe, were consistently applied in all calculations, as well as the "combined correction term."[39,41] The exchange-correlation LDA potential was used in the form proposed by Vosko, Wilk, and Nusair.[42] Experimental lattice constants were used throughout the calculation and the ratios of atomic sphere radii for cation, Te, and empty spheres were taken as 1.25:1.25:1 for CdTe and HgTe and as 1.1:1.25:1 for ZnTe. 220 **k** points were used during the self-consistency procedure which was stopped when relative charge-density changes had decreased below 10^{-4}. All calculations were carried out in a single energy panel, using 5*s*, 5*p*, and 5*d* basis functions for Te and *ns*, *np*, and $(n-1)d$ functions with $n=4$, 5, and 6 for Zn, Cd, and Hg, respectively. Figure 7 shows a schematic layout of the self-consistent bands for all the compounds deduced from the potential-parameter-related quantities V_l, B_l, C_l, and A_l that specify the square-well pseudopotential and the bottom mass center, and top of the l band, respectively.[41] The calculated densities of states of the conduction bands for all three materials are included in the figures in Sec. IV together with the reduced experimental data.

A few general and few specific remarks are in order here concerning the accuracy of our calculations. The LDA is known to fail in predicting a correct energy gap for semiconductors. A procedure is therefore needed which aligns the experimental and theoretical energy scales. This procedure is described in Sec. III B. It remains a question if the LDA fails also in describing a nature of excited states in semiconductors altogether. In assessing our results one should keep in mind the possible sources of errors innate to the LMTO method. It is known that this method with the combined correction term included has, aside from the fourth-order error in $(E-E_v)$, the error of second order in $(E-V_{\mathrm{MTZ}})$, where V_{MTZ} is the average interstitial potential (also marked in Fig. 7). The LMTO method cannot therefore reliably describe bands positioned higher than 1–2 Ry above V_{MTZ}. Hence, we arbitrarily limited the energy range considered to approximately 17 eV above the conduction-band minimum (CBM), i.e., up to ~1.5 Ry above V_{MTZ} (see Fig. 7). It should also be noted that there are not cationic *nd* states in the conduction-band DOS. From chemical trends which are quite evident in Fig. 7 these states are expected to have a non-negligible amplitude for the energies larger than ~0.4 Ry on the scale used in the figure. Therefore, we *a priori* do not expect any good description of the cationic $p\rightarrow d$ transitions for the energy higher than 5–6 eV above the CBM and expect a worse general agreement for Te L_2 and L_3 edges than for Te L_1 edges, because the omission of the cationic *nd* states will cause too large a weight for the Te 5*d* states in eigenvectors. Finally, one should keep in mind that the l decomposition of the DOS, repeatedly used in this paper, is a somewhat

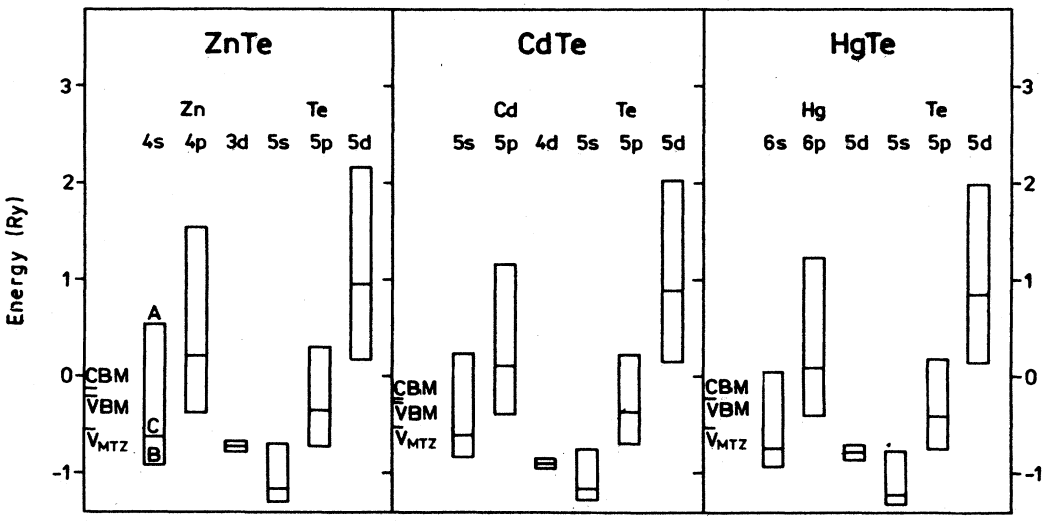

FIG. 7. Schematic layout of the electronic structures of ZnTe, CdTe, and HgTe. The bars depict the extent of the n,l bands as defined by the parameters A (top of the band), C (band center), and B (bottom of the band). The valence-band maximum (VBM), the conduction-band minimum (CBM), and the average interstitial potential V_{MTZ} are also marked.

arbitrary procedure, for it depends to some extent on the choice of atomic radii. This, fortunately, does not seem to be a serious problem. We have compared our results with the unpublished s- and p-like CB DOS for CdTe and HgTe calculated by Lee[43] and Cade, who used a different set of the atomic radii.[44] The results turned out to be almost identical.

B. Absorption spectra calculations

The x-ray-absorption spectrum due to the excitation from the core state $|c\rangle$ is described by the formula[20,21]

$$\mu_0(E)=\frac{2(2j+1)\pi^2e^2\nu}{(2l+1)c\hbar\Omega}E^2 \times\left[\frac{l}{2l-1}f_{c,l-1}(E+E_c)+\frac{l+1}{2l+3}f_{c,l+1}(E+E_c)\right], \quad (6)$$

where Ω is the primitive cell volume, ν the number of atoms in the unit cell, $f_{c,l}(E)=r_{c,l}^2(E)N_l(E)$, $r_{c,l}$ is the dipole transition-matrix element (here assumed to be a constant equal for $l-1$ and $l+1$), and N_l is the partial density of states.

It is assumed here that the initial and final states have infinite lifetimes and thus that their natural width is null. However, an excited electron loses its energy by emitting plasmons or creating electron-hole pairs until it falls near the Fermi level. These processes bring about a finite lifetime and the Lorentzian line shape, which in turn causes a broadening of the spectra. This effect is taken into account by convoluting the DOS spectrum with the Lorentzian function of a width Γ_x that depends on the final-state energy:[20,21]

$$N_l'(E)=\frac{1}{2\pi}\int_{-\infty}^{+\infty}\frac{N_l(E')\Gamma_x(E')}{(E'-E)^2+\Gamma_x(E')^2/4}dE' . \quad (7)$$

$N_l'(E)$ is then used in (6) instead of $N_l(E)$. The core hole has also a finite lifetime caused by radiative or Auger electronic transitions from some occupied higher-energy shells. We include this effect assuming the Lorentzian shape of the initial state (core hole) and calculating the convolution:

$$\mu_1(E)=\int_{-\infty}^{+\infty}\mu_0(E')L(\Gamma,E-E')dE' , \quad (8)$$

where $L(\Gamma,E)=\Gamma/(E^2+\Gamma^2/4)$, with Γ the core-hole width. The values of the core-hole width have been taken from the existing experimental estimations[32] (see Table I). Finally, we take into account the experimental resolution Γ_G:

$$\mu(E)=\frac{1}{\sqrt{2\pi}\Gamma_G}\int_{-\infty}^{+\infty}\exp\left[-\frac{(E-E')^2}{2\Gamma_G^2}\right]\mu_1(E')dE' . \quad (9)$$

Two further difficulties must be overcome before one can compare the theoretical and experimental spectra: alignment of the energy scales and normalization of the spectra. An "*ab initio*" alignment of the energy scales is not possible because our calculations of the electronic structures deliver false information on the energy gaps and no information at all on the chemical shifts; a normalization is an even more difficult problem, the experimental uncertainties being almost impossible to evaluate. To align the energy scales we calculated the first and the second derivatives of the experimental and theoretical absorption spectra, found the position of the inflection points of an absorption edge, and shifted the theoretical spectrum to obtain the same position for these points. Next, the curves were multiplicatively normalized at this point. This arbitrary way of spectrum normalization was chosen out of the conviction that our calculations are most reliable at the bottom of the CB and because the constant-matrix-element approximation precludes any sensible integral normalization procedure.

In the case of metals the steep increase of the absorption coefficient at the edge is directly correlated with the temperature-dependent Fermi-Dirac distribution cutoff multiplied by the product of the unoccupied CB DOS and the transition probability.[15] The inflection point corresponds approximately to the value of binding-energy that lies near the Fermi level.[14] For semiconductors the chemical potential takes over the role of Fermi level. It is situated inside of the forbidden energy gap E_g and only the process of thermal excitation of electrons from the valence band depends upon its position. The resulting temperature-dependent occupancy of the valence- and conduction-band states should participate only as a small correction in the estimated slope of x-ray edges for the room temperature even for HgTe. Hence, the thermal occupancy of the CB DOS was left out of the account in the present study.

To close the discussion of the method of absorption-spectra calculation some remarks seem to be necessary concerning a legitimacy of using the l-decomposed DOS. As was already mentioned in Sec. III A, this decomposition does not depend critically on the relative atomic radii. One could, however, argue, and not without reason, that if we use such a decomposition for the calculation of absorption spectra, we should limit ourselves not only to the sphere surrounding the excited atom but also to this (much smaller) part of it where the initial-state wave functions possess a non-negligible amplitude. This, however, boils down to the problem of the constant-matrix-element approximation. A full *ab initio* calculation of the core transition probability through the k-space integration has not yet, to our best knowledge, been performed. However, from the studies concerning the energy dependence of the matrix element carried out for the purpose of EXAFS interpretation it is known that it remains almost constant within the range of the absorption edge. Hence, similar to the case of the missing *nd* cationic states in the basis set, we expect the constant-matrix-element approximation to influence our results more for higher energies. We do not, however, expect this approximation to influence the slope of the edge itself. Nevertheless, it must be admitted that due to different shapes of the core s and p functions the constant-matrix-element approximation may affect the

(K,L_1) and (L_2,L_3) edges in a different and *a priori* inpredictable way.

For the (L_2,L_3) edges the constant-matrix-element approximation does not actually imply the equality of $r_{c,l-1}$ and $r_{c,l+1}$ in (6). Changing the ratio of them one could correct for the missing *nd* cationic states and improve the agreement between theory and experiment. To our opinion such a procedure would only confuse the issue and was not used here.

IV. DISCUSSION

The absorption coefficient of all studied Te, Cd, and Zn edges is characterized by a rather structureless increase up to the first inflection point at which the first derivative of the total absorption coefficient reaches the most pronounced maximum. Above the point one can observe a complicated fine structure related, as we hope to demonstrate, to the shape of the CB DOS and, for the higher energies, a beginning of the EXAFS structure. Figures 8–13 show the comparison of the convoluted theoretical data with the reduced experimental results. In order to make the comparison more precise and complete, the first derivatives of the spectra are also included.

A. L_1 and K edges

The Te and Cd L_1 edges and Zn K edge correspond to the transitions from s-like core initial states ($n=1$ and $l=0$ for the K edge; $n=2$ and $l=0$ for L_1 edges) to p-like projected components of the CB DOS. The electric dipole transitions ($\Delta p=\pm 1$) should be predominant in the case of Te and Cd L_1 and Zn K edges because, according to Müller *et al.*,[21] the probabilities of the electric quadrupole transitions ($\Delta l=0,\pm 2$) are for these elements negligible.

For all L_1 and K edges very good agreement between theory and experiment has been obtained (see Figs. 8–10). The slope of the experimental absorption edge is very well reproduced by the calculated DOS convolution within a range of more than 5 eV around the inflection point. The height of the reduced experimental data normalized at the inflection point, as well as the energy positions of experimental spectra structures in the 15-eV energy range, also agree quite well with theoretical results. A slight overestimation of the experimental data by calculations at the first maximum can be probably attributed to the constant-matrix-element approximation. The agreement for Zn K and Cd L_1 edges (Fig. 9) is a little worse, as is the agreement in the edge region. In general, the best agreement has been obtained in the energy range in which the influence of the cutoff energy ε can be neglected. As can easily be seen in Fig. 5, the influence of the free-electron model is not negligible for energies higher than $\varepsilon-\Gamma/2$. The theoretical curves around the cutoff energy as decreasing more rapidly than the experimental curves as a result of the convolution procedure near the finite-high-energy calculation limit.

In the case of the Te L_1 edge of HgTe we have compared the experimental results also with Hass CPA band

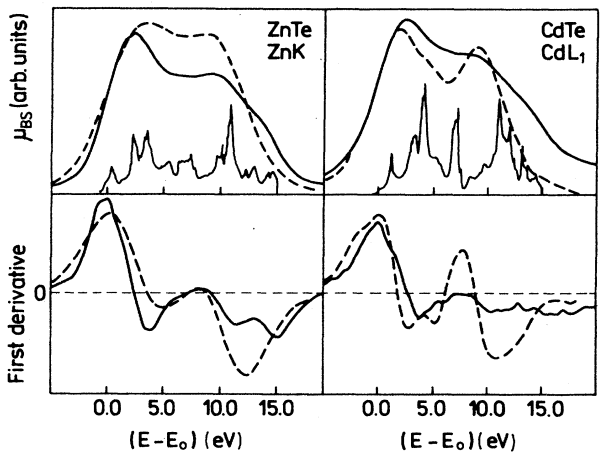

FIG. 9. Reduced experimental spectrum (solid line) with theoretical convolution (dashed line) and their first derivatives for Zn K and Cd L_1 edges in ZnTe and CdTe, respectively. In the insets the calculated projected p-like conduction-band DOS is shown.

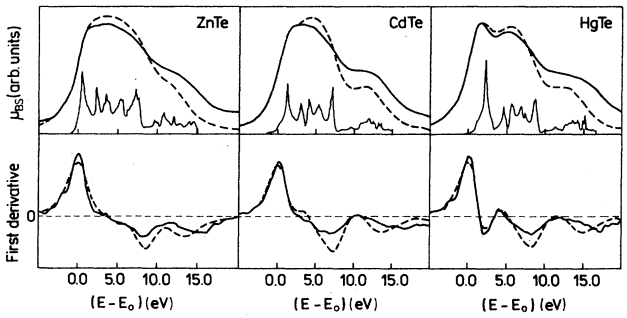

FIG. 8. Reduced experimental spectrum (solid line) with theoretical convolution (dashed line) and their first derivatives for Te L_1 edges in ZnTe, CdTe, and HgTe. In the insets the calculated projected p-like conduction-band DOS is shown.

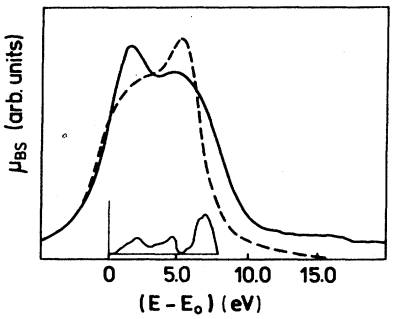

FIG. 10. Reduced experimental spectrum for the Te L_1 edge in HgTe (solid line) and convolution of the conduction-band DOS calculated by Hass (Ref. 45) (dashed line).

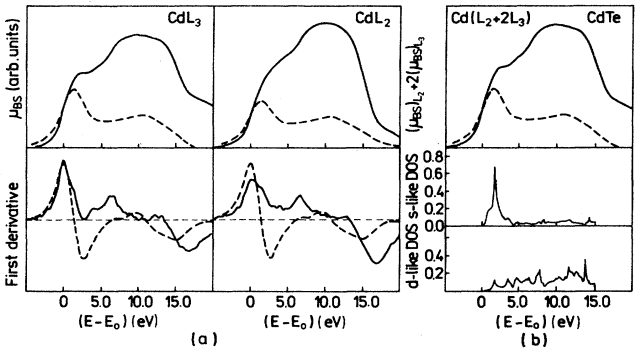

FIG. 11. Reduced experimental spectrum (solid line) and theoretical convolution (dashed line) and their first derivatives for Cd L_2 and L_3 edges in CdTe (left panel) and for comparison the sum of L_2+2L_3 (right panel) with s- and d-like projected conduction-band DOS.

calculations[45] (Fig. 10) carried out up to 8 eV. This comparison shows that our theoretical calculations for HgTe agree better with experiment. In particular, the large DOS calculated by Hass at ~ 6.5 eV does not seem to find an experimental confirmation.

p-like projected CB DOS calculated around the anion (Te) and cations (Zn, Cd, and Hg) in ZnTe, CdTe, and HgTe show significant differences; these differences have been observed in convoluted theoretical DOS as well as in reduced experimental spectra of Te and Cd L_1 edges in CdTe and Te L_1 and Zn K edges in ZnTe. The difference in the shapes of the experimental spectra for Te L_1 and Cd L_1 edges finds its counterpart in the theoretical curves. On the other hand, a general similarity of the Te L_1 edges in all compounds and of the Zn K and Cd L_1 edges is also confirmed by the calculations. The

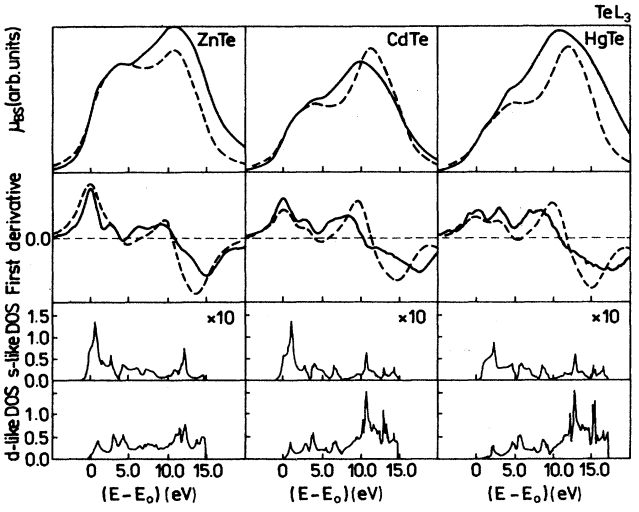

FIG. 12. Reduced experimental spectrum (solid line) with theoretical convolution (dashed line) and their first derivatives for L_3 edges in ZnTe, CdTe, and HgTe. Below, the calculated projected s- and d-like conductivity band DOS are shown.

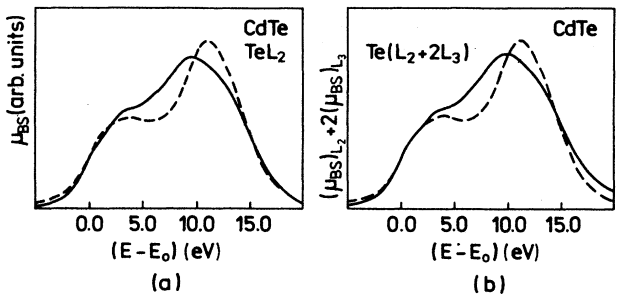

FIG. 13. Reduced experimental (solid line) and theoretical convolution (dashed line) for the Te L_2 edge in CdTe (left panel) and the sum L_2+2L_3 (see text) (right panel).

differences between the cationic and anionic edges are likely an evidence of the mixed covalent-ionic character of he bond between the anion and cation in II-VI compounds, which means a different charge distribution around the anion and cation. The possibility of experimental discrimination between the projected DOS around the anion and cation is an important and unique property of the XAS technique.

The good agreement of theory with experiment discussed above confirms once more the important general result that the projected CB DOS reflects a physical reality in which the atomiclike selection rules are valid. This agreement between the experimental spectra and the convoluted theoretical DOS calculated in the one-electron approximation also indicates that this approximation is sufficient to explain the XANES structures in L_1 and K edges in ZnTe, CdTe, and HgTe.

B. L_2 and L_3 edges

The edges L_2, L_3 of a cation and Te are the result of transitions from p-like core-state components to s- and/or d-like projected CB DOS according to the electric dipole selection rule $\Delta l = \pm 1$. For the reasons discussed by Müller *et al.*,[21] the contribution of the magnetic dipole and quadrupole transitions can be neglected also for these edges. The L_2 and L_3 structures result therefore from the sum of transitions from p-like components to s- and d-like DOS mixed in the ratio $1:\frac{2}{5}$ as defined by formula (6). Looking at the s- and d-like projected CB DOS (Figs. 11 and 12) one can notice a shift of the origin of the d-like DOS to higher energies with respect to the s-like DOS. Thus one can expect that for ZnTe, CdTe, and HgTe and x-ray edge properties close to the inflection point are correlated with transitions from p- to s-like rather than to d-like projected DOS.

Let us first consider the Cd L_3 edge in CdTe. The theoretical calculations reproduce approximately only the position of the first peak which is correlated with the transitions to the s-like projected CB DOS (see Fig. 11). The calculations reproduce neither the steepness at the inflection point nor the intensity in the whole energy range. This total disagreement is almost surely a result of the omission of Cd $4d$ states from the basis set, as discussed in Sec. III A. The differences in the steepness of

the edge are similar to the case of other L_2 and L_3 edges and, to our opinion, result from the core-hole–excited-electron interaction. There are not many experimental papers addressing the problem of the x-ray edge shapes in semiconductors. Evangelisti[48] *et al.* found that many-body effects influence the L_2,L_3 edges in silicon making them more steep. Theoretically forecasted splitting of excitonic energy levels[49] cannot be in general observed due to the short lifetime of core holes. Our results suggest that the influence of many-body effects increases from the Te L_1 edges through the cationic L_1 and K edges to the L_2,L_3 edges, being rather small except in the last case. Right now we do not see any clear explanation of this observation. It is, however, clear that one could improve the agreement between the experimental and theoretical spectra by adjusting the core-level half-width Γ. Such an analysis is currently in progress and their results will be reported in the future.

In the case of the L_2 in L_3 edges of Te in ZnTe, CdTe, and HgTe (Figs. 12 and 13), the agreement of theory with experiment seems to be fairly good, especially if we remember that these edges result from a weighted sum of two diverse *s*- and *d*-like projected DOS contributions. In particular, for ZnTe and CdTe a good agreement is observed in the region close to the inflection point as far as both the height and the shape of experimental and theoretical spectra are concerned. However, the slope of the edges is not reproduced well, similar to what has been observed already for the Cd L_2 edge. The agreement between theory and experiment worsens slightly in passing from HgTe to ZnTe, with the experimental edges being a little steeper than the theoretical ones. The structures observed in the experimental spectra are reproduced well by the theoretical curves. However, the peak at ~ 10 eV that evidently corresponds to the transitions from the *p* core state to *d*-like projected DOS (Fig. 12 and 13) is shifted somewhat (~ 1 eV) upwards in the calculated spectra; this can be clearly seen in the derivative spectrum. The amplitude of the theoretical curves in the case of HgTe and ZnTe is lower than of the experimental ones. Our theoretically calculated band DOS does not distinguish the contribution of the $p_{1/2}$ and $p_{3/2}$ components. Therefore, a really correct comparison of the theoretical results with experiment should be carried out by comparing the total intensity of the transitions from both *p*-like states to both *d*-like components ($d_{3/2},d_{5/2}$), i.e., by comparing the theoretical results with a weighted sum of the experimental L_2 and L_3 edges in the ratio 1:2, as defined by the statistical population of the core-level components. Figure 13 presents this comparison for Te L_2 and L_3 edges in CdTe. It is easy to see that the agreement between theory and experiment is a little improved only in the energy range close to the inflection point. In this case the discrepancy cannot be attributed solely to the effects of the energy cutoff. The most likely explanation of this discrepancy is again, apart from the constant-matrix-element approximation, the omission of the cationic *nd* functions from the basis set, although in an indirect way. This omission causes wrong weights to be attached to the Te 5*p* states with which cationic *nd* states would, when present, strongly hybridize. In particular, we suspect that the upward shift of the ~ 10 eV maximum is caused by just this mechanism. We believe that a two-energy-panel LMTO calculation would bring the theory and experiment into agreement also for L_2 and L_3 edges, for all the features but the edge slope.

V. CONCLUSIONS

On the basis of the preceding discussion, the results obtained in this work can be summarized as follows.

The x-ray near-edge structures for Te and Cd L_1, L_2, and L_3 edges in CdTe, Te L_1 and L_3 edges in ZnTe and HgTe, and the Zn K edge in ZnTe have been measured and analyzed.

The corresponding conduction-band DOS have been calculated using he self-consistent LMTO method.

To allow a direct comparison between theory and experiment, a procedure of experimental data reduction was suggested and applied. The reduced experimental data were directly compared with empty CB DOS up to about 17 eV above the valence-band top.

We have obtained very good agreement between theoretical and experimental results for the Te and Cd L_1 and Zn K edges. This result confirms the ability of the one-particle approximation to explain x-ray near-edge structures for narrow- as well as wide-energy-gap group II-IV compound semiconductors.

Fairly good agreement was also observed for Te L_3 edges in ZnTe, CdTe, and HgTe if one neglects rather small discrepancies in the higher-energy range. We consider this discrepancy to be of the same origin as the large disagreement between theory and experiment found for Cd L_2 and L_3 edges in CdTe: it has to be correlated to the omission of the cationic *nd* states in the CB DOS calculations.

The differences in the slopes of the experimental and theoretical Te and Cd L_2 and L_3 edges seem to be the only indication of any contribution of many-body effects. Their presence, however, in no way hinders the interpretation of the XAS spectra for semiconductors in terms of the one-electron theory.

ACKNOWLEDGMENTS

We would like to thank Dr. A. Balerna, Dr. E. Bernieri, and the technical staff of the Project Wiggler ADONE (PWA) Group of the Laboratori Nazionali di Frascati for their help and hospitality; Dr. P. M. Lee for kindly sending us his unpublished CB DOS results for CdTe and HgTe; and Dr. M. T. Czyżyk for the discussions about the influence of the minimal basis set on calculated optical spectra. One of us (A.K.) gratefully acknowledges the University of Trento, the Research Center of Trento of the National Council of Research (CNR) and the National Institute of Nuclear Physics (INFN) in Frascati for financial support during the initial preparatory stage of this work.

*On leave of absence from the Institute of Physics of the Jagellonian University, Reymonta 4, PL-30-059 Cracow, Poland.
[1]A. Kisiel, M. Zimnal-Starnawska, E. Antonangeli, M. Piacentini, and N. Zema, Nuovo Cimento D **8**, 436 (1986), and references therein.
[2]W. Speier, J. C. Fuggle, R. Zeller, B. Ackermann, K. Szot, F. U . Hillebrecht, and M. Campagna, Phys. Rev. B **30**, 6921 (1984).
[3]W. Speier, R. Zeller, and J. C. Fuggle, Phys. Rev. B **32**, (1985).
[4]C. Laubschat, W. Grentz, and G. Kaindl, Phys. Rev. B **36**, 8233 (1987).
[5]Y. Gao, B. Smandek, T. J. Wagener, J. H. Waever, F. Levy, and G. Margaritondo, Phys. Rev. B **35**, 9357 (1987).
[6]W. Folkers, A. Sawatzky, C. Hass, R. A. de Groot, and F. U. Hillebrecht, J. Phys. C **20**, 4135 (1987).
[7]N. V. Smith, Vacuum **33**, 803 (1983).
[8]D. P. Woodruff, N. V. Smith, P. D. Johnson, and W. A. Royer, Phys. Rev. B **26**, 2943 (1982).
[9]B. Reihl and R. R. Schlittler, Phys. Rev. B **29**, 2267 (1984).
[10]S. L. Hulbert, P. D. Johnson, and M. Weinert, Phys. Rev. B **34**, 3670 (1986).
[11]V. Zlatic, B. Gumhalter, and S. K. Ghatak, Phys. Rev. B **35**, 902 (1987).
[12]A. Simunek and G. Wiech, Phys. Rev. B **30**, 923 (1984).
[13]A. Simunek, G. Drager, W. Czolbe, O. Brummer, and F. Levy, J. Phys. C **18**, 1605 (1985).
[14]L. G. Parratt, Rev. Mod. Phys. **31**, 616 (1959).
[15]E. Noreland, Ark. Phys. **26**, 341 (1964).
[16]V. C. Kostroun, W. Fairchild, C. A. Kukkonen, and J. W. Wilkins, Phys. Rev. B **13**, 3268 (1976).
[17]Raju P. Gupta and A. J. Freeman, Phys. Rev. Lett. **36**, 1194 (1976).
[18]G. D. Mahan, in *Solid State Physics* (Academic, New York, 1974), Vol. 29, p. 75, and extensive references therein.
[19]J. E. Müller, O. Jepsen, O. K. Andersen, and J. W. Wilkins, Phys. Rev. Lett. **40**, 720 (1978).
[20]J. E. Müller, O. Jepsen, and J. W. Wilkins, Solid State Commun. **42**, 365 (1982).
[21]J. E. Müller and J. W. Wilkins, Phys. Rev. B **29**, 4331 (1984).
[22]G. Dalba, P. Fornasini, and E. Burattini, J. Phys. C **16**, L1091 (1983).
[23]T. K. Sham, Phys. Rev. B **31**, 1888 (1984).
[24]B. Poumellec, J. E. Marucco, and B. Tonzelin, Phys. Rev. B **35**, 2284 (1987).
[25]F. Bassani and G. Pastori-Paravicini, *Electronic States and Optical Transition in Solids* (Pergamon, Oxford, 1975).
[26]C. Kunz, *Synchrotron Radiation,* Vol. 10 of *Topics in Current Physics* (Springer, Berlin, 1979), p. 1.
[27]P. A. Lee, P. H. Citrin, P. Eisenberger, and B. M. Kincaid, Rev. Mod. Phys. **53**, 769 (1981).
[28]J. W. McCaffrey and D. A. Papakonstantopoulos, Solid State Commun. **14**, 1055 (1974).
[29]D. A. Papakonstantopoulos, Phys. Rev. Lett. **31**, 1050 (1973).
[30]C. Sagiura and S. Muramatsu, Phys. Status Solidi B **129**, K157 (1985).
[31]E. Burattini, E. Bernieri, A. Balerna, C. Menuccini, R. Rinzivillo, G. Dalba, and P. Fornasini, Nucl. Instrum. Methods A **246**, 125 (1986).
[32]B. K. Teo, *EXAFS: Basic Principles and Data Analysis* (Springer, Berlin, 1986).
[33]L. G. Parratt, Phys. Rev. **567**, 295 (1939).
[34]E. K. Richtmyer, S. W. Barnas, and E. Ramberg, Phys. Rev. **46**, 843 (1934).
[35]K. D. Sevier, *Low Energy Electron Spectroscopy* (Wiley Interscience, New York, 1972).
[36]T. Watanabe, Phys. Rev. **137**, A1380 (1965).
[37]M. A. Blokhin, *The Physics of X-Rays,* 2nd ed. (Mir, Moscow, 1957).
[38]M. O. Krause and J. H. Olivier, J. Phys. Chem. Ref. Data **8**, 329 (1979).
[39]O. K. Andersen, Phys. Rev. B **12**, 3060 (1975).
[40]T. Jarlborg and A. J. Freeman, Phys. Lett. **74A**, 399 (1979).
[41]H. L. Skriver, *The LMTO Method,* Vol. 41 of *Springer Series in Solid State Sciences* (Springer, Berlin, 1984).
[42]S. H. Vosko, L. Wilk, and M. Nusair, Can. J. Phys. **58**, 1200 (1980).
[43]P. M. Lee (private communication).
[44]N. A. Cade and P. M. Lee, Solid State Commun. **56**, 637 (1985).
[45]K. C. Hass, Ph.D. thesis, University of Cambridge, 1984 (unpublished).
[46]B. G. Gokhale, Ph.D. thesis, Paris, 1952 (unpublished) (cited as Ref. 45 in Ref. 35).
[47]J. S. Geiger, R. L. Graham, and J. S. Merritt, Nucl. Phys. **48**, 97 (1963).
[48]F. Evangelisti, F. Patella, R. A. Riedel, G. Margaritondo, P. Fiorini, P. Perfetti, and C. Quaressima, Phys. Rev. Lett. **53**, 2504 (1984).
[49]S. T. Pantelides, Solid State Commun. **16**, 217 (1975).